



The P174L mutation in human Sco1 severely compromises Cox17-dependent metallation but does not impair copper binding.

Paul A Cobine, Fabien Pierrel, Scot C Leary, Florin Sasarman, Yih-Chern Horng, Eric Shoubridge, Dennis R Winge

► **To cite this version:**

Paul A Cobine, Fabien Pierrel, Scot C Leary, Florin Sasarman, Yih-Chern Horng, et al.. The P174L mutation in human Sco1 severely compromises Cox17-dependent metallation but does not impair copper binding.. Journal of Biological Chemistry, American Society for Biochemistry and Molecular Biology, 2006, 281 (18), pp.12270-6. <10.1074/jbc.M600496200>. <hal-00376137>

HAL Id: hal-00376137

<https://hal.archives-ouvertes.fr/hal-00376137>

Submitted on 16 Apr 2009

HAL is a multi-disciplinary open access archive for the deposit and dissemination of scientific research documents, whether they are published or not. The documents may come from teaching and research institutions in France or abroad, or from public or private research centers.

L'archive ouverte pluridisciplinaire **HAL**, est destinée au dépôt et à la diffusion de documents scientifiques de niveau recherche, publiés ou non, émanant des établissements d'enseignement et de recherche français ou étrangers, des laboratoires publics ou privés.

The P174L mutation in human Sco1 severely compromises Cox17-dependent metallation but does not impair copper binding

Paul A. Cobine[†], Fabien Pierrel[†], Scot C. Leary[‡], Florin Sasarman[‡], Yih-Chern Horng[†], Eric A. Shoubridge[‡], Dennis R. Winge^{†*}

From the [†] University of Utah Health Sciences Center, Departments of Medicine and Biochemistry, Salt Lake City, Utah 84132, [‡] Department of Human Genetics and Montreal Neurological Institute of McGill University, 3801 University Street, Room 660, Montreal, Quebec H3A 2B4

Running title: Cox17-mediated metallation of human Sco1

* Address correspondence to: Dennis Winge, University of Utah Health Sciences Center, Salt Lake City, Utah 84132; Tel: 801-585-5103; Fax: 801-585-5469; Email: dennis.winge@hsc.utah.edu or Eric Shoubridge Tel: 514-398-1997; Fax: 514-3998-1509; Email: eric@ericpc.mni.mcgill.ca

Sco1 is a metallochaperone that is required for copper delivery to the Cu_A site in the CoxII subunit of cytochrome *c* oxidase. The only known missense mutation in human Sco1, a P174L substitution in the copper-binding domain, is associated with a fatal neonatal hepatopathy; however, the molecular basis for dysfunction of the protein is unknown. Immortalized fibroblasts from a *SCO1* patient show a severe deficiency in cytochrome *c* oxidase activity that is partially rescued by overexpression of P174L Sco1. The mutant protein retains the ability to bind Cu(I) and Cu(II) normally when expressed in bacteria, but Cox17-mediated copper transfer is severely compromised both *in vitro* and in a yeast cytoplasmic assay. The corresponding P153L substitution in yeast Sco1 is impaired in suppressing the phenotype of cells harboring the weakly functional C57Y allele of Cox17; however, it is functional in *sco1Δ* yeast when the wild-type *COX17* gene is present. Pulse-chase labeling of mitochondrial translation products in *SCO1* patient fibroblasts showed no change in the rate of CoxII translation, but a specific and rapid turnover of CoxII protein in the chase. These data indicate that the P174L mutation attenuates a transient interaction with Cox17 that is necessary for copper transfer. They further suggest that defective Cox17-mediated copper metallation of Sco1, and subsequent failure of Cu_A site maturation, is the basis for the inefficient assembly of the cytochrome *c* oxidase complex in *SCO1* patients.

Cytochrome *c* oxidase (CcO) is the terminal enzyme of the energy transducing respiratory chain in mitochondria of eukaryotes and in certain prokaryotes. The enzyme catalyzes the reduction of molecular oxygen and couples this reduction with proton translocation across the inner membrane to generate the membrane potential used to synthesize ATP. The mammalian enzyme consists of 13 subunits, three of which, CoxI, CoxII and CoxIII, are mitochondrially-encoded and form the catalytic core. Structurally conserved domains within subunits I and II contain the copper and heme cofactors that are essential for the catalytic competence of the holoenzyme (1). CoxI contains two heme A moieties, one of which interacts with a mononuclear copper site forming a heterobimetallic site, designated heme A₃-Cu_B. Two additional copper ions exist in a cysteine-bridged, binuclear, mixed valent center in CoxII designated Cu_A. Assembly of individual structural subunits into a functional holoenzyme complex within the mitochondrial inner membrane requires over thirty accessory factors (2).

Isolated CcO deficiency, one of the most commonly recognized causes of respiratory chain defects in humans, is associated with a wide spectrum of clinical phenotypes (3,4), and autosomal recessive mutations have been identified in six nuclear genes that encode CcO assembly factors in these patients,(3-9). Two such factors, *SCO1* and *SCO2* encode metallochaperones that play a role in the copper ion metallation of the Cu_A site in CoxII. This step in CcO assembly requires a single Sco

protein in yeast (Sco1), but both Sco proteins are essential in humans. Recent studies with immortalized fibroblasts from *SCO1* and *SCO2* patients suggest that Sco1 and Sco2 have non-overlapping but cooperative functions in the maturation of the Cu_A site (10), although their specific molecular roles in CcO assembly have yet to be defined.

Sco1 was first implicated in copper delivery to CcO by the observation that the respiratory deficient phenotype of a *cox17-1* yeast mutant was suppressed by overexpression of *SCO1* (11). Deletion of the *SCO1* gene in yeast cells produces a respiratory phenotype attributable to a lack of CcO activity. Structural studies of Sco1 show that it has a globular domain with a thioredoxin fold consisting of a central four stranded β sheet covered with flanking helices that protrude into the mitochondrial intermembrane space (IMS) (12). Two other notable features of Sco proteins are a conserved pair of cysteinyl residues in a CxxxC motif and a conserved histidyl residue. These residues are spatially close in the apo-Sco1 structure in a solvent-exposed pocket (12).

Sco1 is capable of binding a single Cu(I) ion (18). X-ray absorption spectroscopy suggests that the Cu(I) is ligated via two sulfur donors and a nitrogen. Mutation of either the Cys or His residues abolishes Cu(I) binding and results in a non-functional CcO complex (18). Cox17 is the likely physiological copper donor to Sco1 (19) consistent with the postulate that Sco1 mediates Cu(I) transfer from Cox17 to CoxII. Sco proteins also bind Cu(II) (13). The Cu(II) site resembles a type II Cu(II) site with a higher coordination number than the three-coordinate Cu(I) site. A D238A substitution in yeast Sco1 abrogated Cu(II) coordination and led to a nonfunctional protein. These data suggest that both Cu(I) and Cu(II) binding are critical for normal Sco1 function (13).

Mutations in either h*SCO1* or h*SCO2* result in pronounced CcO deficiency and lead to different, early onset, fatal clinical phenotypes (4,6,7,14). *SCO2* mutations are associated with neonatal encephalocardiomyopathy, whereas *SCO1* patients present with neonatal hepatic failure and ketoacidotic coma. These distinct clinical phenotypes are not a result of tissue-specific expression of the two genes, as *SCO1*

and *SCO2* are ubiquitously expressed and exhibit a similar expression pattern in different human tissues (4).

All reported *SCO2* patients carry an E140K missense mutation on one allele, and are either homozygous for this mutation or are compound heterozygotes. Homozygous patients have a delayed onset of the disease pathology and a more prolonged course of disease as compared to heterozygotes (14). *SCO1* mutations have only been identified in a single pedigree in which the reported patients carried a nonsense mutation on one allele and a P174L missense mutation on the second allele (5). Both the E140K and P174L substitutions are adjacent to the CxxxC sequence motif.

Human Sco1 and Sco2 are nonfunctional in yeast *sco1 Δ* cells (15); however, a chimeric protein consisting of 158 residues from the N-terminus of yeast Sco1 fused to a C-terminal segment of hSco1, but not hSco2, is functional. A P174L substitution was found to attenuate its function (15,16), although the CcO deficiency in yeast *sco1 Δ* cells harboring the mutant yeast/human Sco1 chimera could be rescued for growth on a nonfermentable carbon by the addition of 0.2% CuSO₄ (16). This suggests that P174L Sco1 retains some residual function; however, the molecular defect in Sco1 function that results from this amino acid substitution remains unknown. The present study was therefore initiated to investigate whether copper binding is defective in the P174L mutant Sco1. We report that although copper binding is wild-type in the mutant Sco1, its metallation by Cox17 is severely compromised.

MATERIALS AND METHODS

Yeast strains and human cell lines-All yeast strains used were in the W303 background (MAT a, *ade2-1*, *his3-1,15*, *leu2,3,112*, *trp1-1*, *ura3-1*). Cells were cultured with glucose, raffinose, or galactose as carbon sources as described (19). DNA transformations were performed using a lithium acetate protocol.

Primary cell lines from control *SCO1* and *SCO2* patient skin fibroblasts were immortalized and cultured as previously

described (10). Preparation and supplementation of the growth media with copper histidine (Cu-His) was also as described elsewhere (10). *Plasmids*- The construction of YEp-*GALI*-h*SCO1* and pHis-h*SCO1* were described previously (13). The P174L mutation was introduced into these plasmids using the QuickChange™ site-directed mutagenesis kit (Stratagene, La Jolla, CA). A pRS413 vector (YCp) expressing yeast *SCO1* with a C-terminal HA tag sequence under the control of the *MET25* promoter with a *CYC1* terminator was used as a template to generate the P153L mutation. The entire insert was then subcloned into a pRS423 vector (YEpl). The *MET25* promoter was also replaced with the 350 upstream base pairs that make up the natural *SCO1* promoter in the centromeric vector. The plasmid encoding Cyb2-C57Y Cox17 was described previously (17). DNA sequences were confirmed prior to use.

Wild-type h*SCO1* cloned into the Gateway-modified retroviral expression vector pLXSH was used as a template to generate the P174L point mutant using the QuickChange™ mutagenesis. The fidelity of the resultant construct was confirmed by sequencing. Phoenix amphotropic cells (Dr. G. Nolan, Stanford University) were used to transiently produce and package all individual human cDNA constructs. Subsequent infection and selection of fibroblast cell lines were done as previously described (10).

Protein Purification-Recombinant human and yeast Sco1 proteins were purified from BL21 (DE3) transformants harboring pHis-h*SCO1* (His-tagged *SCO1* or mutant *SCO1*) as described previously (18). Yeast transformants with YEp-*GALI*-h*SCO1* were cultured in raffinose medium to an $A_{600\text{ nm}}$ of 0.6. Galactose was then added to induce expression of the His-tagged Sco1. Cells were harvested after 5 h and lysates were prepared by use of a French press. Nickel-NTA Superflow (Qiagen) was used for the purification of the His-tagged Sco1 proteins from clarified samples.

Spectroscopic analyses - Absorption spectra were recorded with a Beckman DU640 spectrophotometer. X-band EPR spectra were obtained on a 9 GHz Bruker EMX spectrometer. All samples were run at 77K in a liquid nitrogen

finger dewar. Spin quantitation was determined relative to a 0.5 mM CuEDTA standard. Luminescence was monitored on a Perkin Elmer fluorimeter with excitation wavelength of 300 nm and emissions were scanned from 350 to 700 nm. Excitation slit of 5 nm and emission slit of 15 nm and a 350 nm bandpass filter were used. The copper concentration of the protein samples was measured using a Perkin Elmer (AAAnalyst 100) atomic absorption spectrophotometer or a Perkin Elmer Optima (3100XL) ICP spectrometer. Circular dichroism spectra were recorded on an Aviv 62DS spectrometer at room temperature using a 0.3 cm cuvette path length and are the average of three scans.

Assays-A bathocuproine sulfonate (BCS) assay was used to determine the Cu(I) content of the protein samples. The appearance of a Cu(BCS)₂ complex was measured by monitoring the absorbance at 483 nm using a molar extinction coefficient of 12,250 cm⁻¹M⁻¹. Protein was quantified by amino acid analysis after hydrolysis in 5.7 N HCl at 110 °C *in vacuo* on a Beckman 6300 analyzer.

Mitochondrial translation studies-Cells were pulse-labelled for 60 min at 37° C in methionine-free DMEM containing 200 µCi/ml [³⁵S]methionine and anisomycin (100µg/ml), a reversible cytosolic translation inhibitor, and chased for up to 17.5 hr in regular DMEM. Total cellular protein (50 µg) was resuspended in loading buffer containing 93 mM Tris-HCl, pH 6.7, 7.5% glycerol, 3.5% SDS, 0.25 mg bromophenol blue/ml and 3% mercaptoethanol, sonicated for 3–8 s, loaded and run on 12–20% polyacrylamide gradient gels.

Immunoblot Analysis of yeast proteins-Protein (10–50 µg) from the mitochondrial fraction was electrophoresed on a 15% SDS-PAGE gel system and transferred to nitrocellulose (Bio-Rad Laboratories). Membranes were blocked in 1x phosphate-buffered saline (50 mM Na₂PO₄, 100 mM NaCl, pH 7.0), 0.01% Tween 20, and 10% milk solution prior to detection with appropriate antibodies and visualization with Pierce chemiluminescence reagents using a horseradish peroxidase-conjugated secondary antibody. Antiserum to porin (Por1) was from Molecular Probes. Rabbit anti-Sco1 antiserum was generated as described previously (18).

Immunoblot analysis of human proteins-

Immortalized human fibroblasts and myoblasts were differentially permeabilized using digitonin in order to generate mitochondrially-enriched fractions, and subsequently solubilized in phosphate buffered saline containing 1.5% lauryl maltoside supplemented with complete protease inhibitor cocktail (Roche) (10). Equal amounts of protein were fractionated on 12% SDS-PAGE gels, and transferred to nitrocellulose. Membranes were blotted with polyclonal antisera raised against human Sco1 and CoxII, and a monoclonal anti-Por1 antibody (Calbiochem). Following incubation with the relevant secondary antibody, immunoreactive proteins were detected by luminol-enhanced chemiluminescence (Pierce).

Miscellaneous - Protein concentration, CcO and citrate synthase activities in human cell lines were measured as described elsewhere (10).

RESULTS

Immortalized fibroblasts from a *SCO1* patient with the P174L substitution exhibit a severe deficiency in CcO, which is reflected in both low residual enzyme activity and low steady-state levels of CoxII protein (Figs. 1A,C). Transduction of patient fibroblasts with a retroviral virus overexpressing *SCO1* completely restored wild-type CcO activity (Fig. 1A) (10), while over-expression of the P174L mutant *SCO1* only partially rescued the CcO deficiency (Fig. 1A). These changes in CcO activity were accompanied by parallel increases in the steady-state levels of CoxII protein (Fig. 1C). Residual CcO activity in P174L-overexpressing *SCO1* patient fibroblasts could be further increased by supplementing the growth media with Cu-His (Fig. 1A), an effect that was not attributable to altered levels of Sco1 protein (data not shown). These data demonstrate that the P174L mutant Sco1 retains sufficient residual function to allow for some assembly of the CcO holoenzyme.

Although the reduced CcO activity in *SCO1* patient cells could be partly due to reduced Sco1 protein levels (10) (Fig. 1C), the inability of overexpressed P174L Sco1 mutant to fully restore CcO activity argues that some aspect of its function is impaired. We previously showed that overexpression of either

Sco protein in the reciprocal patient background exerts a dominant-negative effect on CcO activity (10) that was dependent on the Cu(I)-binding Cys residues in Sco1 (13). To evaluate whether the P174L substitution affected this genetic interaction between Sco1 and Sco2, we overexpressed either the wild-type or the P174L mutant Sco1 in *SCO2* patient fibroblasts. Both wild-type and mutant Sco1 proteins exerted a comparable dominant-negative effect on residual CcO activity and residual CoxII protein levels (Fig. 1B,D). This phenotype was robust, and could not be perturbed by the presence of Cu-His in the growth media. These results suggest that at least a fraction of over-expressed P174L Sco1 is metallated in *SCO2* fibroblasts.

To further evaluate the molecular defect in the P174L mutant Sco1, N-terminal truncates of wild-type and P174L human Sco1 were expressed and purified (13) to characterize their copper-binding properties. Both wild-type Sco1 and the P174L mutant protein eluted from gel filtration in fractions corresponding to monomeric molecules, and each contained 0.9 mol equiv. of copper (Table I). Dialysis of the copper-containing proteins overnight in 1 mM EDTA/1 mM DTT resulted in only a slight depletion of bound copper; both wild-type and P174L Sco1 proteins retained 0.8 mol equiv. bound copper. The copper binding avidity to wild-type and P174L Sco1 was therefore similar. Titration of the proteins with varying levels of the Cu(I) specific chelator bathocuproine sulfonate (BCS) revealed a similar BCS concentration dependency in Cu(I) depletion, further suggesting that Cu(I) coordination was similar in the two proteins (Fig. 2).

The Cu(II) content, assessed by the quantity of copper that is not BCS-titratable, was 0.4 mol equiv. for both the wild-type and P174L Sco1 (Table I). Absorption spectroscopy of purified wild-type Sco1 revealed the expected transitions of the Cu(II) chromophore in the visible spectral region with maxima at 360 and 480 nm (Fig. 3A). The P174L Sco1 exhibited the same transitions, confirming that the mutant Sco1 binds Cu(II) in a manner analogous to that of the wild-type protein. Comparable Cu(II) coordination between wild-type and P174L Sco1 was further confirmed by electron paramagnetic resonance spectroscopy; both proteins exhibited

similar hyperfine splittings of the g_z component of the Cu(II) signal (Fig. 3B). Far UV circular dichroism revealed that the wild-type and mutant Sco1 proteins exhibited similar bulk structure, with comparable ellipticity in the two proteins, suggesting that the P174L substitution fails to grossly perturb the tertiary conformation of the protein (Fig. 4). Collectively, these data strongly suggest that the molecular defect caused by the P174L substitution does not result from aberrant copper binding.

We demonstrated previously that Cox17 is a Cu(I) donor to yeast and human Sco1 using both *in vitro* and *in vivo* approaches (13,19). To investigate whether P174L Sco1 can be metallated by Cox17, purified wild-type and mutant Sco1 proteins were initially tested in an *in vitro* transfer assay. CuCox17 exhibits a characteristic luminescence at 580 nm that, upon addition of apo-Sco1, leads to an attenuation in emission due to Cu(I) transfer (19). The addition of apo-hSco1 to CuCox17 resulted in a rapid attenuation in the Cox17 luminescence (Fig. 5A). Subsequent purification of hSco1 by Ni-NTA chromatography and quantitation of bound copper confirmed that quenching of Cox17 luminescence was attributable to copper transfer (Fig. 5C). The eluate contained only hSco1, so the observed copper transfer between Cox17 and hSco1 was likely mediated by transient interactions between the two proteins (Fig. 5D). The specificity of the Cu(I) transfer from Cox17 to hSco1 was verified by using a C57Y mutant Cox17 that we previously demonstrated fails to transfer Cu(I) to yeast Sco1 (19). As before, incubation of hSco1 with the yeast C57Y mutant Cox17 failed to show any Cu(I) transfer, as assessed by the lack of diminution in the Cox17 emission spectrum (Fig. 5A).

In contrast to wild-type hSco1, incubation of CuCox17 with P174L hSco1 failed to show either a diminution in CuCox17 emission or Cu(I) transfer after recovery of the mutant protein (Fig. 5B,C). Increasing the concentration of CuCox17 five-fold in the reaction resulted in limited transfer of Cu(I) to the purified P174L hSco1 sample to a final stoichiometry of 0.4 mol eq. (data not shown). As expected, incubation of the yeast C57Y mutant Cox17 and the P174L hSco1 failed to show any Cu(I) transfer (Fig. 5B).

The inability of P174L hSco1 to be metallated by CuCox17 was further confirmed using the yeast cytosolic assay (19). Constructs encoding the globular domains of hSco1 and P174L hSco1 as His-tag fusions were expressed from the *GALI* promoter on a high copy YEp plasmid. The proteins accumulated in the yeast cytoplasm as they lacked their usual mitochondrial targeting sequence and transmembrane domains. Purification of hSco1 from the cytoplasm of cells co-expressing Cox17 and cultured in synthetic complete medium resulted in recovery of hSco1 with a bound copper content of 0.9 mol equiv. (Fig. 6). In contrast, co-expression of Cox17 and P174L hSco1 yielded only residual copper (0.1 mol equiv.) in the purified mutant Sco1, consistent with the above *in vitro* data.

The failure of Cox17 to metallate P174L Sco1 may in part explain the very low steady-state levels of CoxII protein observed in *SCO1* patient fibroblasts (Fig. 1C). To evaluate the effects of the P174L substitution on CoxII expression at the protein level, pulse-chase labeling experiments of mitochondrial translation products were conducted. Rates of CoxII protein synthesis were comparable in control and *SCO1* patient fibroblasts; however, there was a dramatic reduction in the stability of nascent CoxII in *SCO1* patient fibroblasts during the chase (Fig. 7A). The temporal loss of CoxII preceded similar reductions in the levels of CoxI and CoxIII, the two other mitochondrially-encoded structural subunits (Fig. 7B). Radiolabelled CoxII was undetectable eight hours post-chase in *SCO1* patient fibroblasts (Fig. 7B). In contrast, roughly 20% of the total radiolabelled CoxII pool from the pulse remained in control fibroblasts, an amount that persisted until the final time point at 17.5h (Fig. 7B).

Pro174 is a conserved residue in eukaryotic Sco proteins. To determine whether a corresponding mutation in yeast *SCO1* attenuated function, a P153L substitution was engineered in yeast *SCO1* and expressed on a centromere-based vector from its natural promoter. Yeast cells lacking Sco1 are respiratory deficient and lack CcO activity. Transformation of *scd1Δ* cells with a mutant *SCO1* encoding the P153L substitution

suppressed the growth phenotype of *sco1Δ* cells on ethanol/glycerol (Fig. 8) and restored wild-type oxygen consumption, suggesting that the P153L mutant protein was functional. As a second test of functionality, we evaluated the ability of mutant *SCO1* to suppress the respiratory deficiency of *cox17-1* cells. This partially functional allele of Cox17 contains a C57Y substitution, and glycerol growth of *cox17-1* cells can be restored by overexpression of *SCO1* (11). To test for potential suppression by mutant Sco1, we used *cox17Δ* cells harboring a plasmid expressing C57Y Cox17 as a fusion protein with the Cyb2 heme domain (designated Cox17-1*) to allow for its efficient accumulation within the IMS. Mutant *cox17-1* cells with either wild-type or the P153L mutant *SCO1* were plated on glycerol-containing medium. Whereas wild-type *SCO1* reversed the growth phenotype on glycerol/ethanol when expressed from a YCp plasmid under its natural promoter (Fig. 9A), complementation of the phenotype by the P153L Sco1 required a much higher level of expression of the protein (Fig. 9A). Western analysis revealed that the wild-type and mutant protein accumulated to similar extents (Fig. 9B), ruling out the possibility that the inactivity of P153L Sco1 arose from reduced levels of the mutant protein.

The ability of Sco1 to restore glycerol growth of *cox17Δ* cells was dependent on the presence of C57Y Cox17. In the absence of C57Y Cox17, suppression of *cox17Δ* cells requires *SCO1* overexpression and the addition of exogenous copper to the growth medium. Partial suppression of *cox17Δ* cells by overexpression of P153L Sco1 occurred in the presence of exogenous copper added to the growth medium (Fig. 9A).

DISCUSSION

The present study clearly demonstrates that the P174L substitution in hSco1 does not affect the ability of the protein to bind and retain Cu(I) or Cu(II), but rather impairs its ability to receive copper from the metallochaperone Cox17. Although the P174L variant has wild-type copper-binding properties, its function *in vivo* is severely compromised as evidenced by

the pronounced CcO assembly defect in *SCO1* patient tissues and fibroblasts (6,10). Overexpression of the mutant *SCO1* in patient fibroblasts only partially suppresses the CcO deficiency, consistent with a loss of function mutation.

Using *in vitro* and *in vivo* copper transfer assays we previously showed that Cox17 transfers Cu(I) to both Sco1 and Cox11 in yeast (19), and that hCox17 transfers Cu(I) to hSco1 (13). The specificity of this transfer reaction is highlighted by a mutant form of Cox17 (C57Y) that fails to transfer Cu(I) to Sco1 despite normal Cu(I) binding and transfer to Cox11. The P174L substitution in Sco1 also appears to perturb the interaction with Cox17, as its metallation in both the *in vitro* assay and the *in vivo* yeast cytosolic assay was at residual levels.

The failure of Cox17 to metallate P174L hSco1 *in vitro* could be partially reversed by substantially increasing Cox17 concentrations in the transfer reaction, suggesting that overexpression of either P174L Sco1 or hCox17 might rescue CcO activity in *SCO1* patient fibroblasts. Although we demonstrated partial rescue of the CcO phenotype by overexpressing P174L Sco1, we did not observe any rescue by overexpressing Cox17, even though immunoblot analysis of whole cell extracts indicated that we were able to overexpress it 2-3 fold using retroviral expression vectors (data not shown). Cox17 is, however, distributed between the cytoplasm and the mitochondrial IMS (20), and it is possible that this experiment did not result in a significant enough increase of Cox17 concentration in this compartment to promote copper loading of Sco1 in patient cells.

An attenuation of the interaction between Cox17 and the mutant hSco1 is further supported by the observation that P153L Sco1 in yeast is impaired in suppressing the phenotype of *cox17-1* cells harboring the C57Y substitution in Cox17. Whereas overexpression of wild-type Sco1 suppresses the growth phenotype of *cox17-1* cells on ethanol/glycerol, expression of P153L *SCO1* from a YCp vector fails to restore CcO activity. Interestingly, the P153L substitution in yeast Sco1 does not apparently compromise the interaction with Cox17 as seriously as the P174L mutation in the human protein. No respiratory

phenotype is observed in *sco1Δ* cells expressing the P153L Sco1.

The exact nature of the Cox17-Sco1 interaction is not yet clear. We have failed to observe an interaction using affinity purification of Sco1 from both *in vivo* and *in vitro* copper transfer assays (19), suggesting that Cox17 donates Cu(I) through ligand exchange reactions in a transient protein-protein interaction. We propose that this complex is attenuated by the C57Y substitution in Cox17 and by the P174L substitution in Sco1. This could arise if Pro174 is part of the interaction interface, or alternatively, if P174L alters Sco1 conformation. It is conceivable that Sco1 exists in two subconformational states, an open conformer receptive to Cu(I) binding and a closed state poised for transfer to CoxII. The failure of Cox17 to donate Cu(I) to P174L Sco1 could arise if Sco1 existed in the closed conformer, mimicking the Cu-loaded state.

We cannot rule out the possibility that the P174L substitution impairs copper transfer from Sco1 to CoxII: however, the fact that the CcO deficiency in *SCO1* patient fibroblasts is partially reversed by the addition of exogenous copper salts to the culture medium (10) suggests that it is more likely a copper loading problem. Although the exact mechanism of copper suppression of the mutant hSco1 remains unresolved, the exogenous copper could bypass Cox17 in the metallation of Sco1 within the IMS using another metallochaperone. There are at least two candidates that might be able to fulfill this role, Cox19 and Cox23, both of which share the conserved C_{X9}C motif originally identified in Cox17 (21).

The most important ramification of the P174L mutation in Sco1 is the failure to incorporate newly synthesized CoxII into the holoenzyme complex. This stalls the CcO assembly process, resulting in accumulation of a subassembly and the production of a limited amount of active holoenzyme (22). Mitochondria contain a AAA protease system in the inner membrane that is responsible for the quality control of inner membrane proteins (23), rapidly turning over newly synthesized mitochondrial proteins that are not incorporated into nascent enzyme complexes. While it is therefore not surprising to find that nascent

mitochondrially-encoded Cox subunits are degraded more rapidly in cells with a CcO assembly defect than in controls, *SCO1* patient cells are unique in that the turnover of newly synthesized CoxII occurs more rapidly than that of CoxI and CoxIII. We have not observed this specificity in other cell lines from patients with other isolated CcO assembly defects and similarly low residual CcO activity (unpublished observations). This suggests that it is the inefficient maturation of the Cu_A site that results in the disproportionately rapid degradation of apo-CoxII molecules, further emphasizing that CoxII is the molecular target of Sco1.

Overexpression of P174L Sco1 as well as wild-type hSco1 exerts a dominant negative effect on CcO activity in *SCO2* patient fibroblasts, an effect that we previously showed depends on intact copper binding in the wild-type protein (13). Mutant Sco1 must be at least partly copper-loaded as it retains limited function. It is possible that even a small pool of metallated Sco1 would be sufficient to cause the dominant negative effect in *SCO2* patient cells, as these cells have very low steady-state levels of Sco2 protein. Alternatively, the P174L substitution could stabilize a conformation mimicking the copper-loaded state. Future studies will address the effect of the P174L substitution on the conformation of Sco1 and its interaction with Sco2.

Acknowledgements: This work was supported by a grant ES 03817 from the National Institutes of Environmental Health Sciences, NIH to D.R.W. and grants from MDA and CIHR to E.A.S. E.A.S. is an International Scholar of the HHMI and a senior investigator of the CIHR. S.C.L. holds a post-doctoral fellowship from the CIHR.

REFERENCES

1. Tsukihara, T., Aoyama, H., Yamashita, E., Tomizaki, T., Yamaguchi, H., Shinzawa-Itoh, K., Hakashima, R., Yaono, R., and Yoshikawa, S. (1995) *Science* **269**, 1069-1074
2. Tzagoloff, A., and Dieckmann, C. L. (1990) *Microbiological Rev.* **54**, 211-225
3. Zhu, Z., Yao, J., Johns, T., Fu, K., De Bie, I., Macmillan, C., Cuthbert, A. P., Newbold, R. F., Wang, J., Chevrette, M., Brown, G. K., and Shoubridge, E. A. (1998) *Nat. Genet.* **20**, 337-343
4. Papadopoulou, L. C., Sue, C. M., Davidson, M. M., Tanji, K., Nishion, I., Sadlock, J. E., and al., e. (1999) *Nature Genetics* **23**, 333-337
5. Valnot, I., Von Kleist-Retzow, J.-C., Barrientos, A., Gorbatyuk, M., Taanman, J.-W., Mehaye, B., Rustin, P., Tzagoloff, A., Munnich, A., and Rotig, A. (2000) *Human Molecular Genetics* **9**, 1245-1249
6. Valnot, I., Osmond, S., Gigarel, N., Mehaye, B., Amiel, J., Cormier-Daire, V., Munnich, A., Bonnefont, J.-P., Rustin, P., and Rotig, A. (2000) *Am. J. Hum. Genet.* **67**, 1104-1109
7. Jaksch, M., Ogilvie, I., Yao, J., Kortenhaus, G., Bresser, H.-G., Gerbitz, K.-D., and Shoubridge, E. A. (2000) *Hum. Mol. Genet.* **9**, 795-801
8. Antonicka, H., Mattman, A., Carlson, C. G., Glerum, D. M., Hoffbuhr, K. C., Leary, S. C., Kennaway, N. G., and Shoubridge, E. A. (2002) *Am. J. Hum. Genet.* **72**, 101-114
9. Mootha, V. K., Lepage, P., Miller, K., Bunkenborg, J., Reich, M., Hjerrild, M., Delmonte, T., Vvilleneuve, A., Sladek, R., Xu, F., Mitchell, G. A., Morin, C., Mann, M., Hudson, T. J., Robinson, B., Rioux, J. D., and Lander, E. S. (2004) *Proc. Natl. Acad. Sci. USA* **100**, 605-610
10. Leary, S. C., Kaufman, B. A., Pellechia, G., Gguercin, G.-H., Mattman, A., Jaksch, M., and Shoubridge, E. A. (2004) *Hum. Mol. Genet.* **13**, 1839-1848
11. Glerum, D. M., Shtanko, A., and Tzagoloff, A. (1996) *J. Biol. Chem.* **271**, 20531-20535
12. Williams, J. C., Sue, C., Banting, G. S., Yang, H., Glerum, D. M., Hendrickson, W. A., and Schon, E. A. (2005) *J. Biol. Chem.* **280**, 15202-15211
13. Horng, Y.-C., Leary, S. C., Cobine, P. A., Young, F. B. J., George, G. N., Shoubridge, E. A., and Winge, D. R. (2005) *J. Biol. Chem.* **280**, 34113-34122
14. Jaksch, M., Horvath, R., Horn, N., Auer, D. P., Macmillan, C., Peters, J., Gerbitz, K.-D., Kraegeloh-Mann, I., Muntau, A., and al., e. (2001) *Neurology* **57**, 1440-1446
15. Paret, C., Ostermann, K., Krause-Buchholz, U., Rentzsch, A., and Rodel, G. (1999) *FEBS Lett* **447**, 65-70
16. Paret, C., Lode, A., Krause-Buchholz, U., and Rodel, G. (2000) *Biochem. Biophys. Res. Comm.* **279**, 341-347
17. Maxfield, A. B., Heaton, D. N., and Winge, D. R. (2004) *J. Biol. Chem.* **279**, 5072-5080
18. Nittis, T., George, G. N., and Winge, D. R. (2001) *J. Biol. Chem.* **276**(45), 42520-42526
19. Horng, Y. C., Cobine, P. A., Maxfield, A. B., Carr, H. S., and Winge, D. R. (2004) *J. Biol. Chem.* **279**, 35334-35340
20. Beers, J., Glerum, D. M., and Tzagoloff, A. (1997) *J. Biol. Chem.* **272**, 33191-33196
21. Barros, M. H., Johnson, A., and Tzagoloff, A. (2004) *J. Biol. Chem.* **279**, 31943-31947
22. Williams, S. L., Valnot, I., Rustin, P., and Taanman, J.-W. (2004) *J. Biol. Chem.* **279**, 7462-7469
23. Leonhard, K., Herrmann, J. M., Stuart, R. A., Mannhaupt, G., Neupert, W., and Langer, T. (1996) *EMBO J.* **15**, 4218-4229

Table I

Cu(I) and Cu(II) binding stoichiometry of human Sco1 and Sco1 P174L

Protein samples were quantified for total copper by ICP-OES analysis. The Cu(II) content was calculated by subtracting the BCS reactive Cu(I) (incubation with 25 mM BCS for 30 min) from the total copper amount and confirmed by quantitation of the Cu(II) EPR signal. Protein was quantified by amino acid analysis. (n=3)

	Total Cu/protein mol equiv.	Cu(II)/protein mol equiv.	Post-dialysis Total Cu/protein mol equiv.	Post-dialysis Cu(II)/protein mol equiv.
hSco1	0.94 ± 0.1	0.40 ± 0.05	0.80 ± 0.1	0.40 ± 0.07
hSco1 P174L	0.95 ± 0.1	0.44 ± 0.05	0.78 ± 0.2	0.42 ± 0.05

Figure legends

Figure 1. **Complementation analysis in *SCO1* and *SCO2* patient cell lines transduced with retroviral expression vectors expressing either wild-type *SCO1* or P174L *SCO1*.** A,B) CcO activity, expressed as a percentage of control (n=3-11), in untransduced *SCO1* and *SCO2* patient fibroblasts (baseline) and in cells overexpressing either wild-type or P174L Sco1. Baseline and retroviral-overexpressing cells were grown in either the absence or presence of 30 μ M copper-histidine (Cu-His) for 7 days prior to analysis. C,D) Immunoblot analysis of expression of Sco1 and CoxII in control and patient fibroblast (panel C) and myoblast (panel D) lines in untransduced cells (-) and in cells overexpressing either wild-type Sco1 or P174L Sco1. Porin served as an internal loading control.

Figure 2. **Competition of hSco1 and hSco1 P174L with the Cu(I)-chelator BCS.** Cu(BCS)₂ complex was measured by monitoring the absorbance at 483 nm using a molar extinction coefficient of 12,250 cm⁻¹M⁻¹. 20 μ M of hSco1 (bold line) and hSco1 P174L (dashed line) were incubated with varying concentrations of BCS and the Cu(BCS)₂ complex was quantified after 10 min. Representative data are shown of n=3.

Figure 3. **Spectroscopic characterization of the Cu(II) site in hSco1 and hSco1 P174L.** A) Absorption spectra of purified hSco1 (bold line) and hSco1 P174L (dashed line). B) EPR spectra of purified hSco1 (top) and hSco1 P174L (bottom) with each sample present at a final copper concentration of 0.5 mM. The spectra were recorded at 77K at a power setting of 19.8 mW and a modulation amplitude of 4.0 G. Representative data are shown of n=3.

Figure 4. **Far UV circular dichroism spectra of purified hSco1 and hSco1 P174L.** The concentrations of purified hSco1 (bold line) and hSco1 P174L (dashed line) were 25 μ M.

Figure 5. **Cox17-mediated copper transfer to hSco1 and hSco1 P174L.** CuCox17 or CuCox17-C57Y present at 20 μ M was incubated with 50 μ M apo hSco1 or hSco1 P174L for the *in vitro* transfer reaction. A) The luminescence of CuCox17 before (solid line, top panel) and after the addition of apo-hSco1 (dashed line, top panel) is shown. The bottom panel shows the luminescence of CuCox17-C57Y before (solid line) and after the addition of apo-hSco1 (dashed line). B) The luminescence of CuCox17 before (solid line, top panel) and after the addition of apo-hSco1 P174L (dashed line, top panel) is shown. The emission of CuCox17-C57Y before (solid line, bottom panel) and after the addition apo-hSco1 P174L (dashed line, bottom panel) is shown. C) The copper content of His-tagged hSco1 and hSco1 P174L after purification by Ni-NTA chromatography (eluate fractions) is shown by white bars (n=3). The unbound fraction containing only Cox17 is shown by black bars D) SDS-PAGE of the eluate fractions containing hSco1 and hSco1 P174L.

Figure 6. **Copper transfer assay from Cox17 to hSco1 and hSco1 P174L in yeast cytoplasm.** Yeast cells containing plasmids expressing yeast Cox17 and the His-tagged soluble domains of either hSco1 or hSco1 P174L were cultured as described in Material and Methods. The His-tag hSco1 proteins were purified on Ni-NTA and the copper content of the eluted fractions are shown (n=3). The purity of the hSco1 in the eluted fractions was determined by SDS-PAGE (inset).

Figure 7. **Synthesis and turnover of mitochondrial CcO subunits in *SCO1* fibroblasts.** A) Fibroblasts from the *SCO1* patient and a control were pulse-labeled for one hour with [³⁵S]methionine in the presence of a reversible inhibitor of cytoplasmic translation (anisomycin), followed by chase in regular medium for various intervals of time (shown, in hours, at the top of the figure), to assess the rate of synthesis and the stability of mitochondrial Cox subunits. Ten of the 13 mitochondrially-encoded structural subunits of the

oxidative phosphorylation complexes are indicated at the left of the figure: “CO”, subunits of CcO; “ND”, subunits of complex I; cyt b, subunit of complex III; “ATP6”, subunit of complex V. B) The temporal decrease of the three mitochondrially-encoded subunits of CcO in control patient fibroblasts is expressed as percentage of radioactive counts incorporated following a 0.2 h chase period. The end points of the experiment (0.2h pulse, 17.5 h chase were assessed in five independent experiments, while the refined time course for the chase portion of the experiment was done singly.

Figure 8. Complementation of *sco1*Δ yeast cells growth defect on non-fermentable carbon sources by ySco1 P153L. Serial dilutions of *sco1*Δ cells containing an empty plasmid (VEC) or a plasmid expressing either SCO1 or SCO1 P153L under the control of the natural promoter were spotted onto selective plates containing 2% glucose or 2% lactate - 2% glycerol with and without 1 mM CuSO₄.

Figure 9. Suppression of *cox17-1* cells by yeast Sco1 P153L. A) Transformants of *cox17*Δ cells were spotted onto selective plates containing 2% glucose or 2% lactate - 2% glycerol with and without 1mM CuSO₄ as follows: empty plasmid (VEC), a plasmid encoding Cyb2-C57Y Cox17 (Cox17-1*) in combination with YCp or YEp plasmids encoding either wild-type Sco1-HA (strip A) or Sco1-HA P153L (strip B) under the control of the endogenous *SCO1* (*sco*) or *MET25* promoters (*met*). B) Immunoblot analysis confirmed equal protein levels of Sco1-HA or Sco1-HA P153L in the *cox17-1* cells. Mitochondrial protein, Por1, is shown as a loading control.

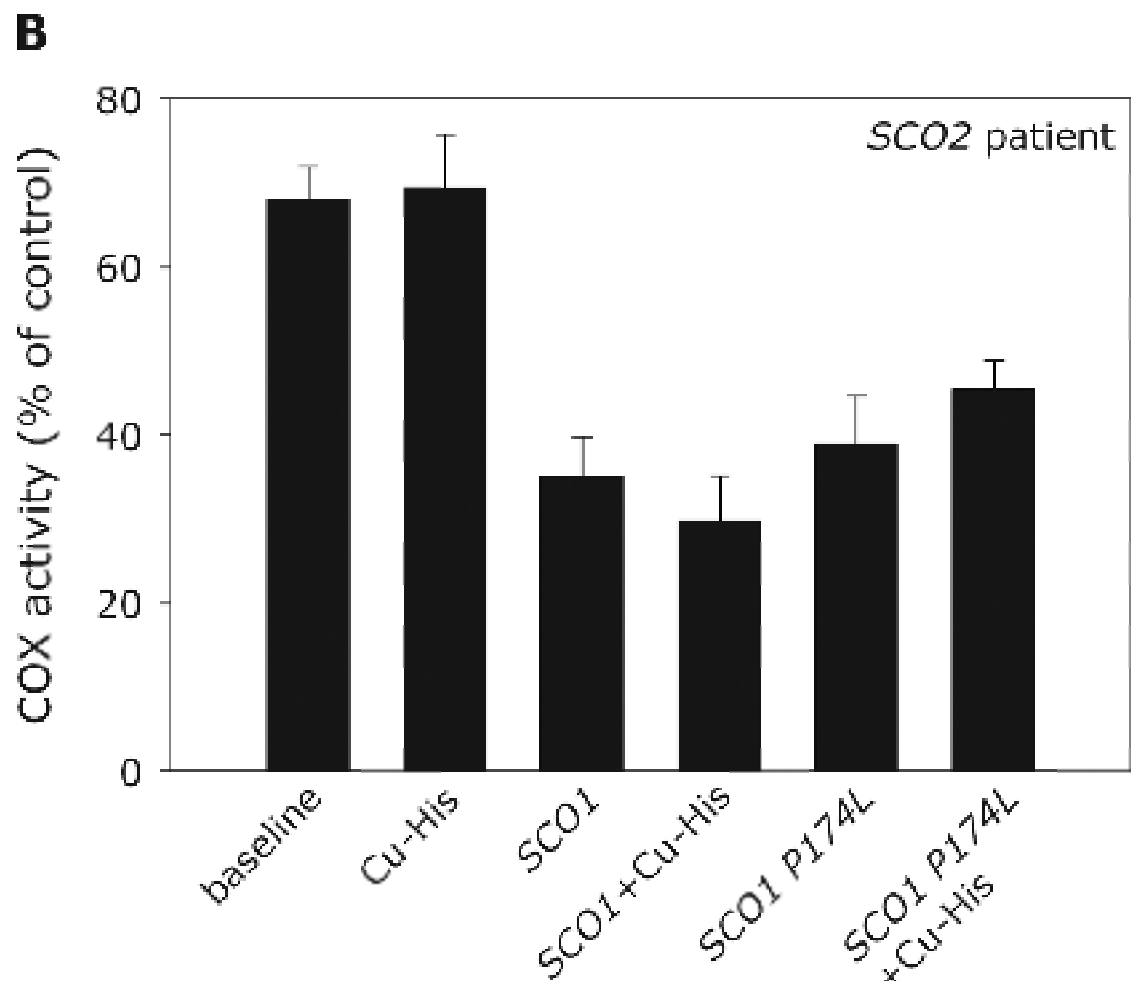
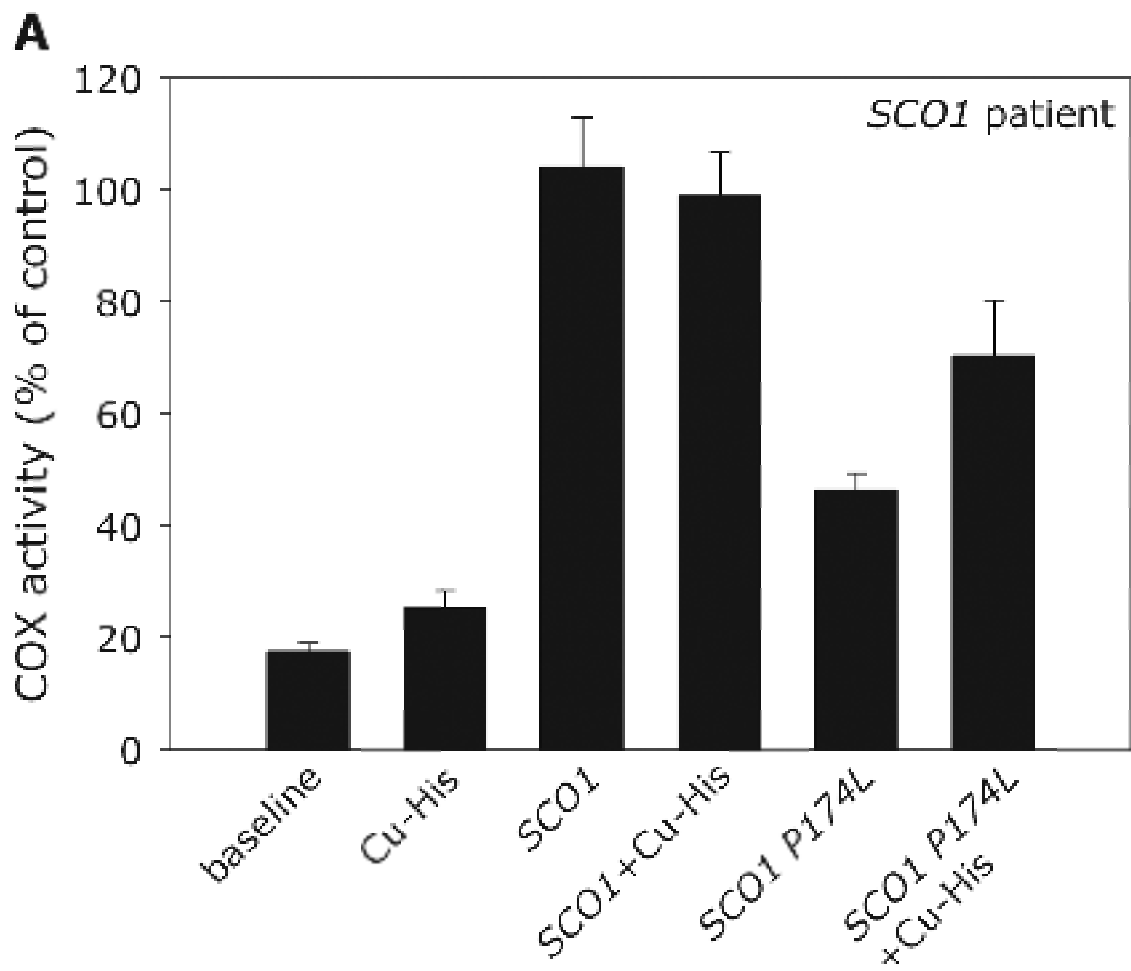
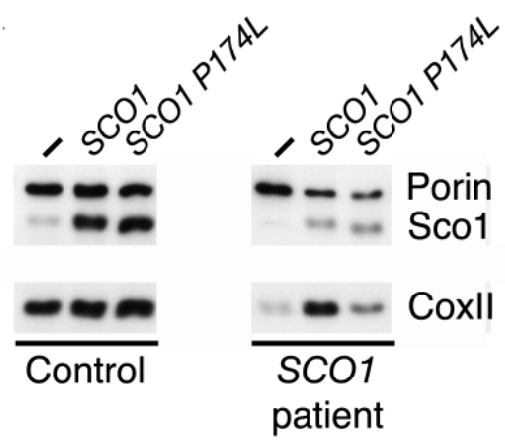


Figure1

C



D

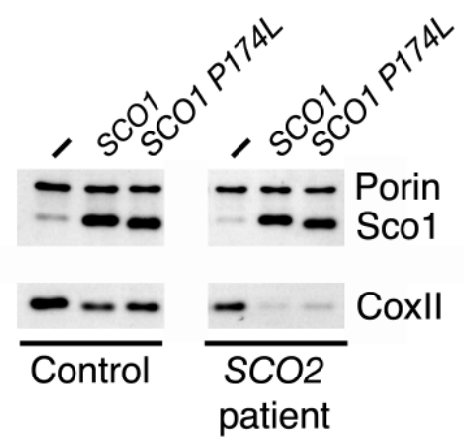


Figure1

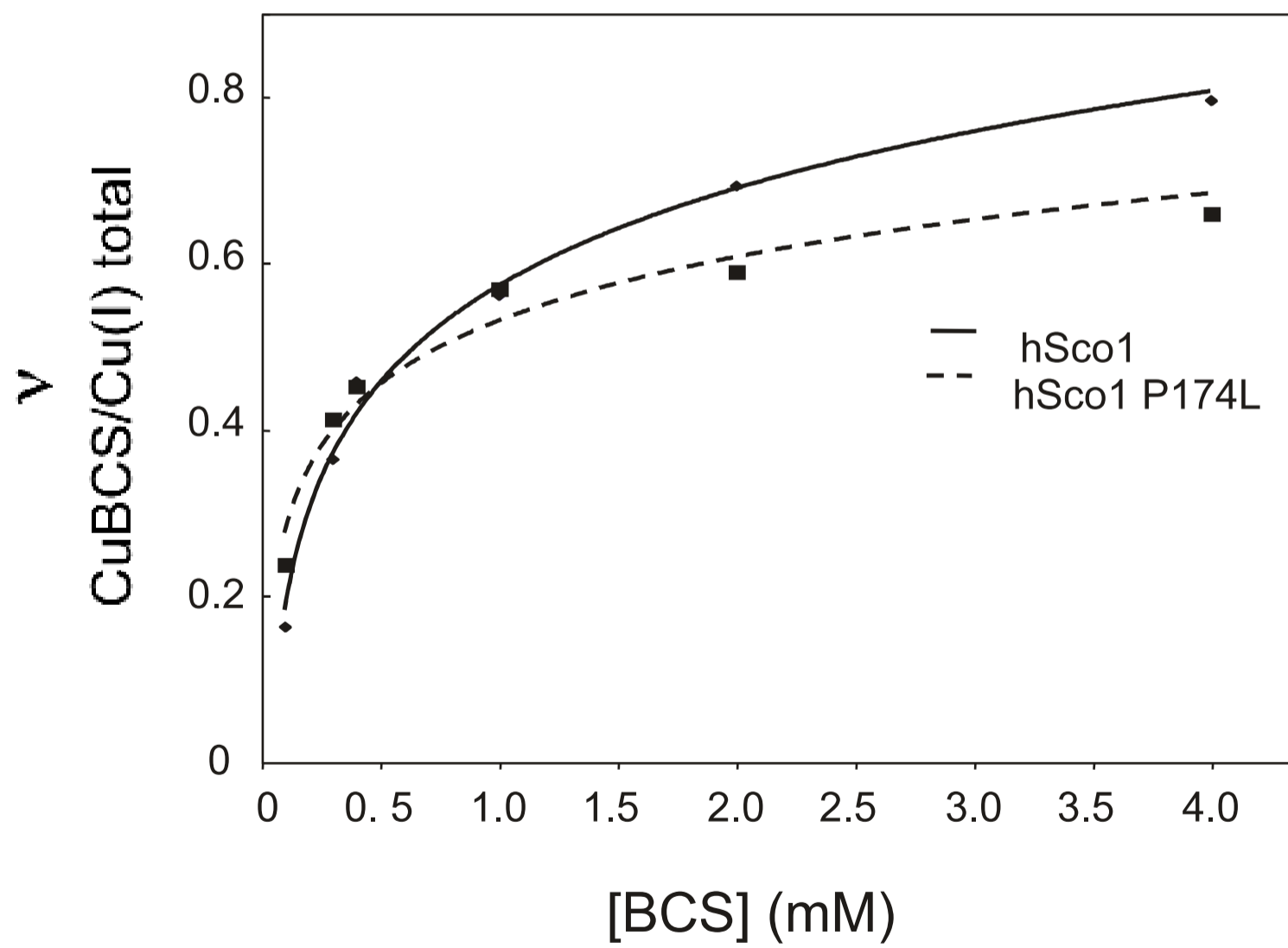


Fig.2

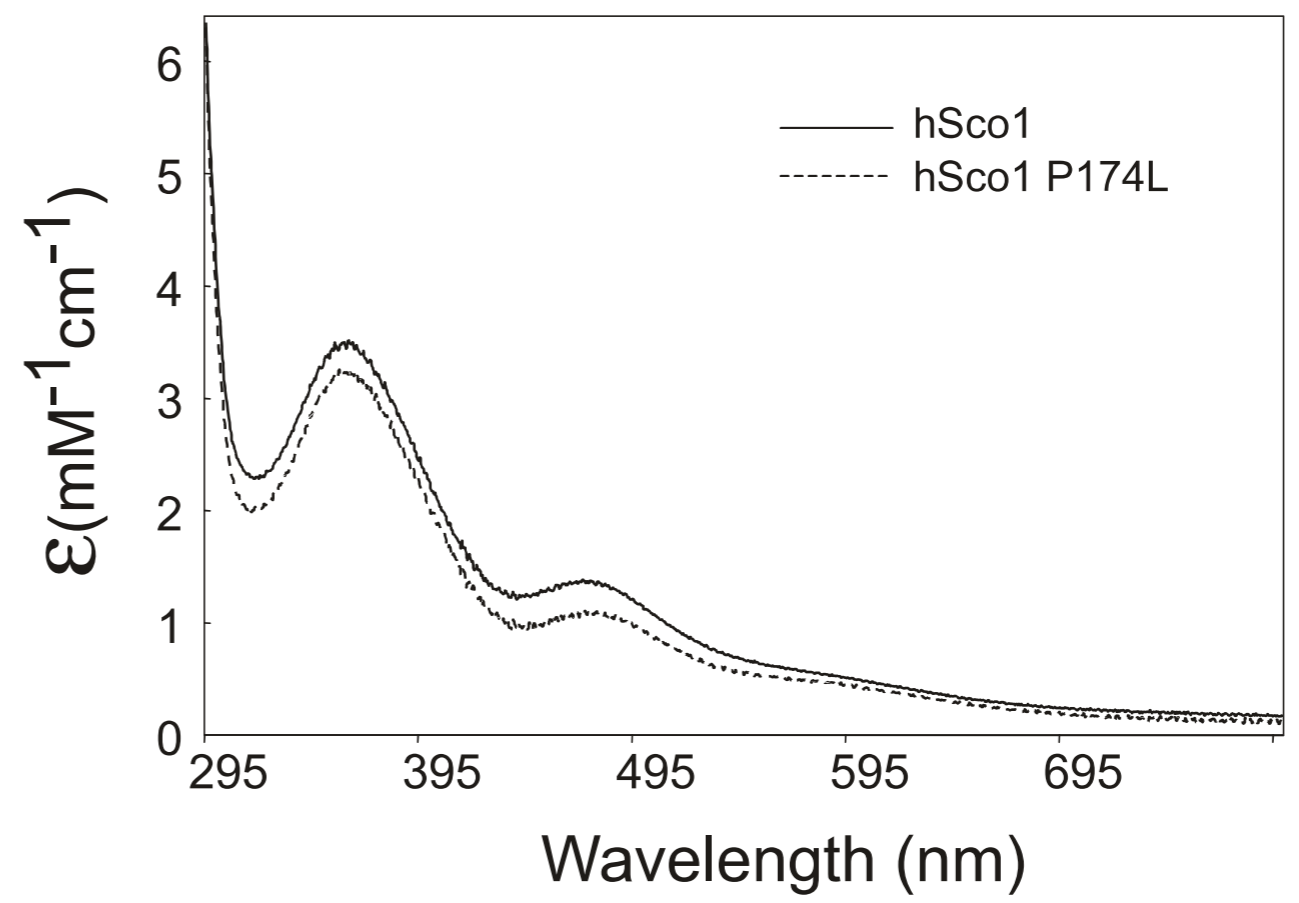


Fig.3A

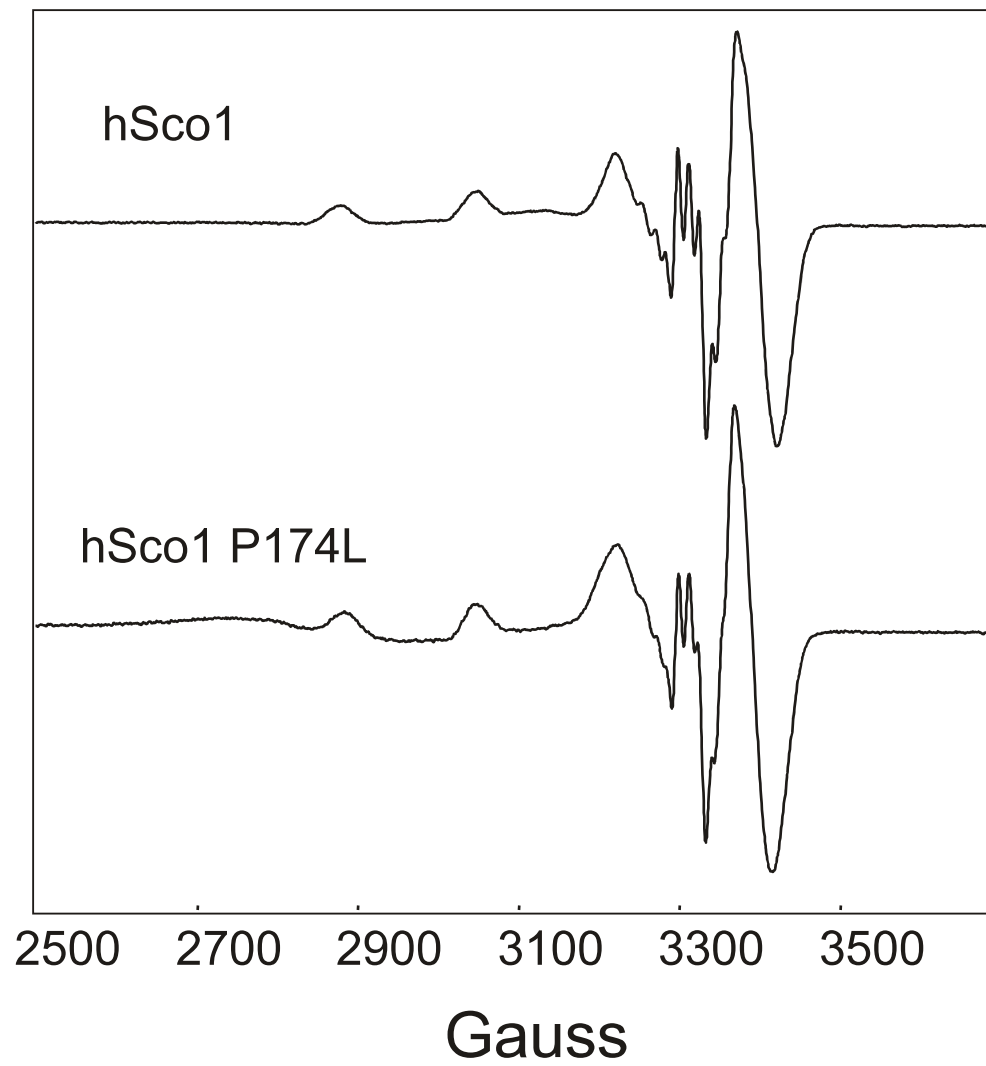


Fig.3B

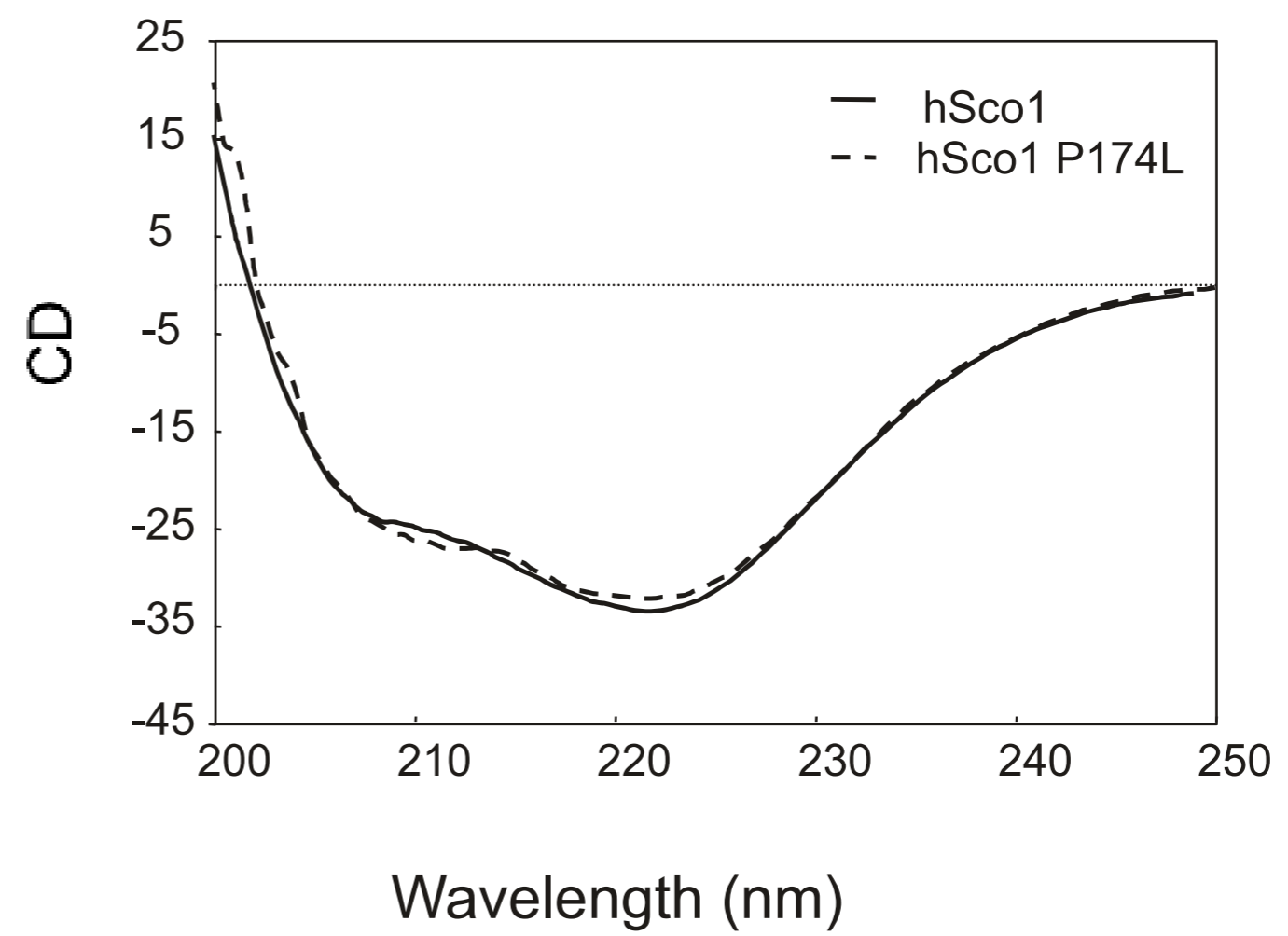


Fig.4

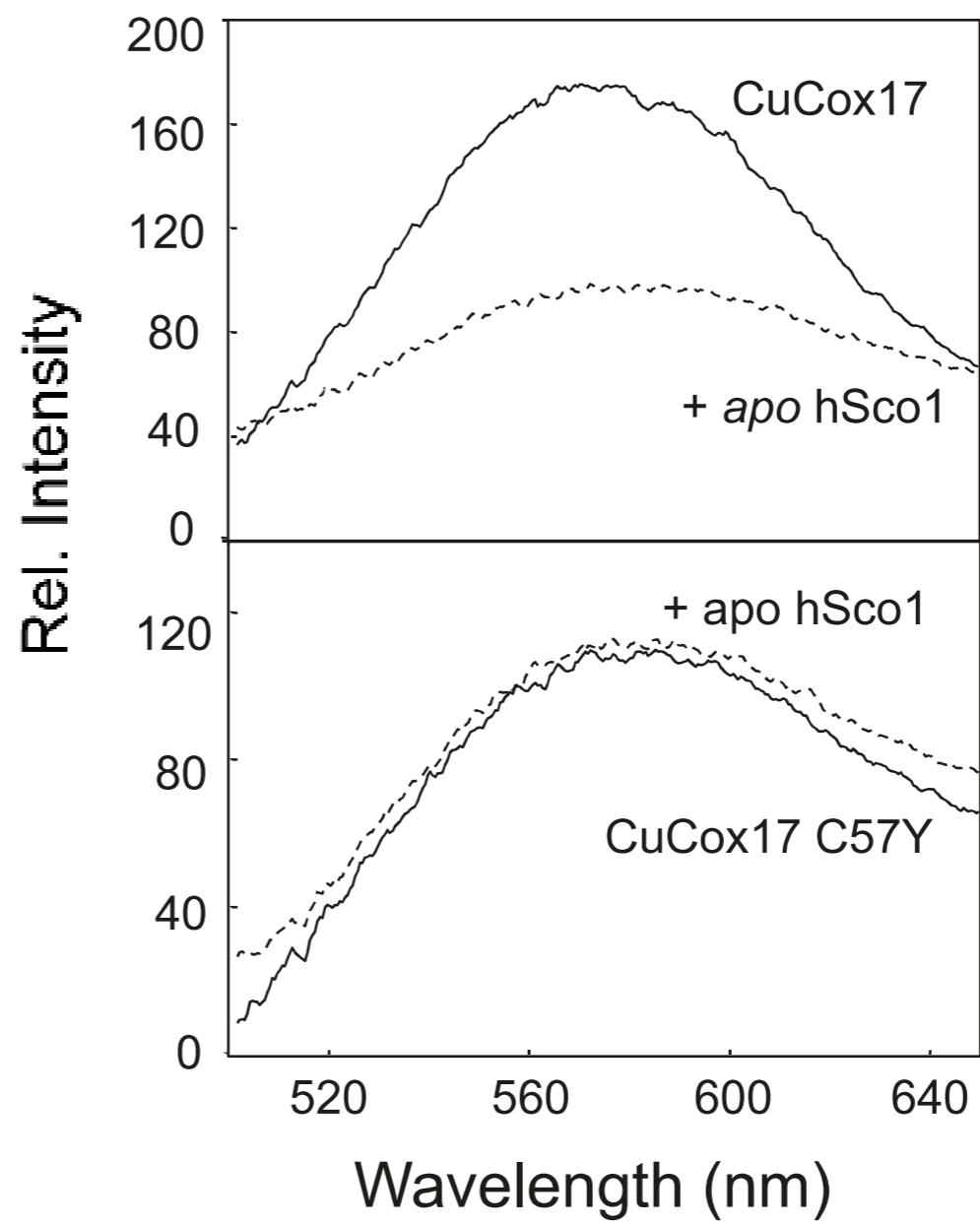


Fig.5A

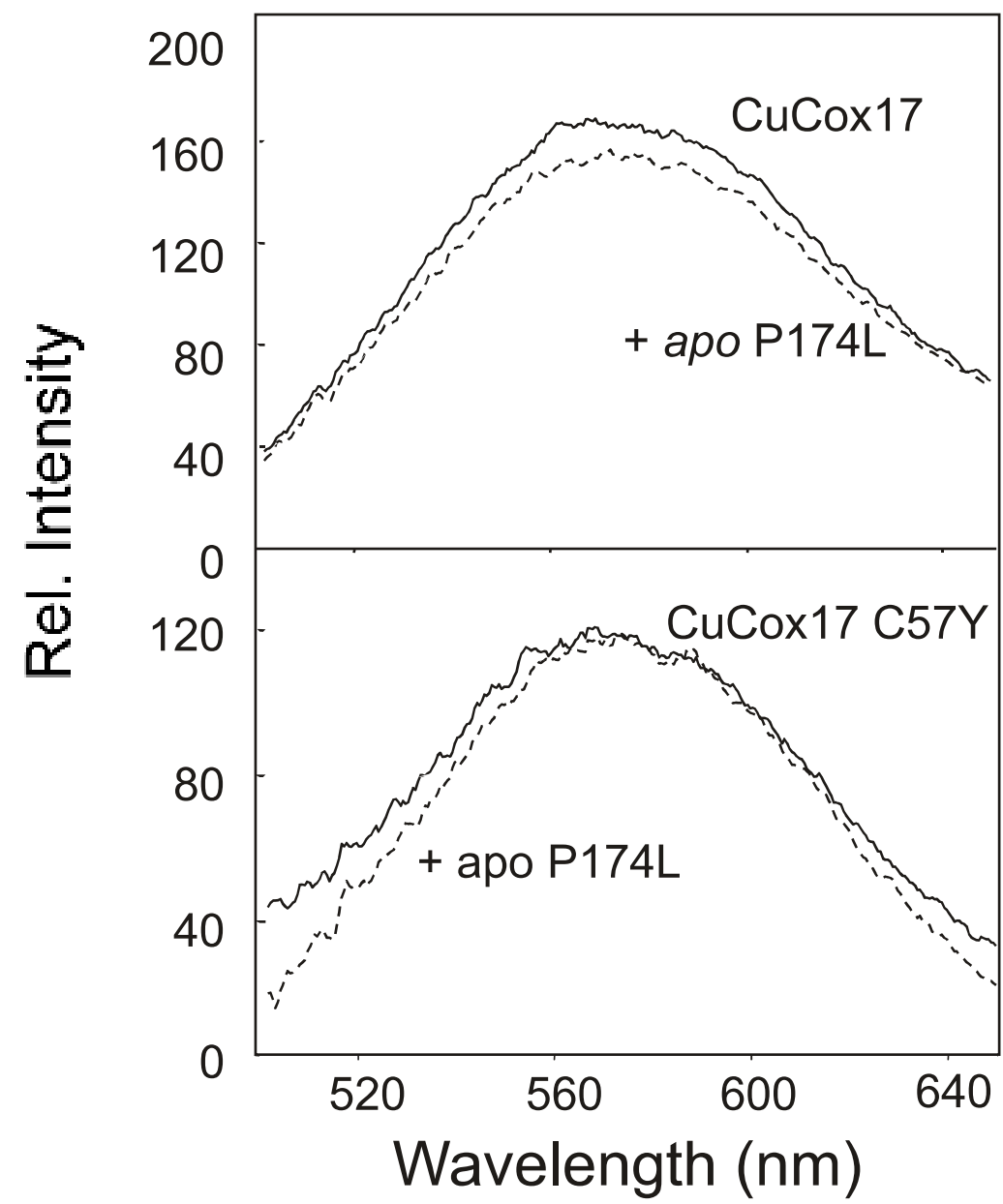


Fig.5B

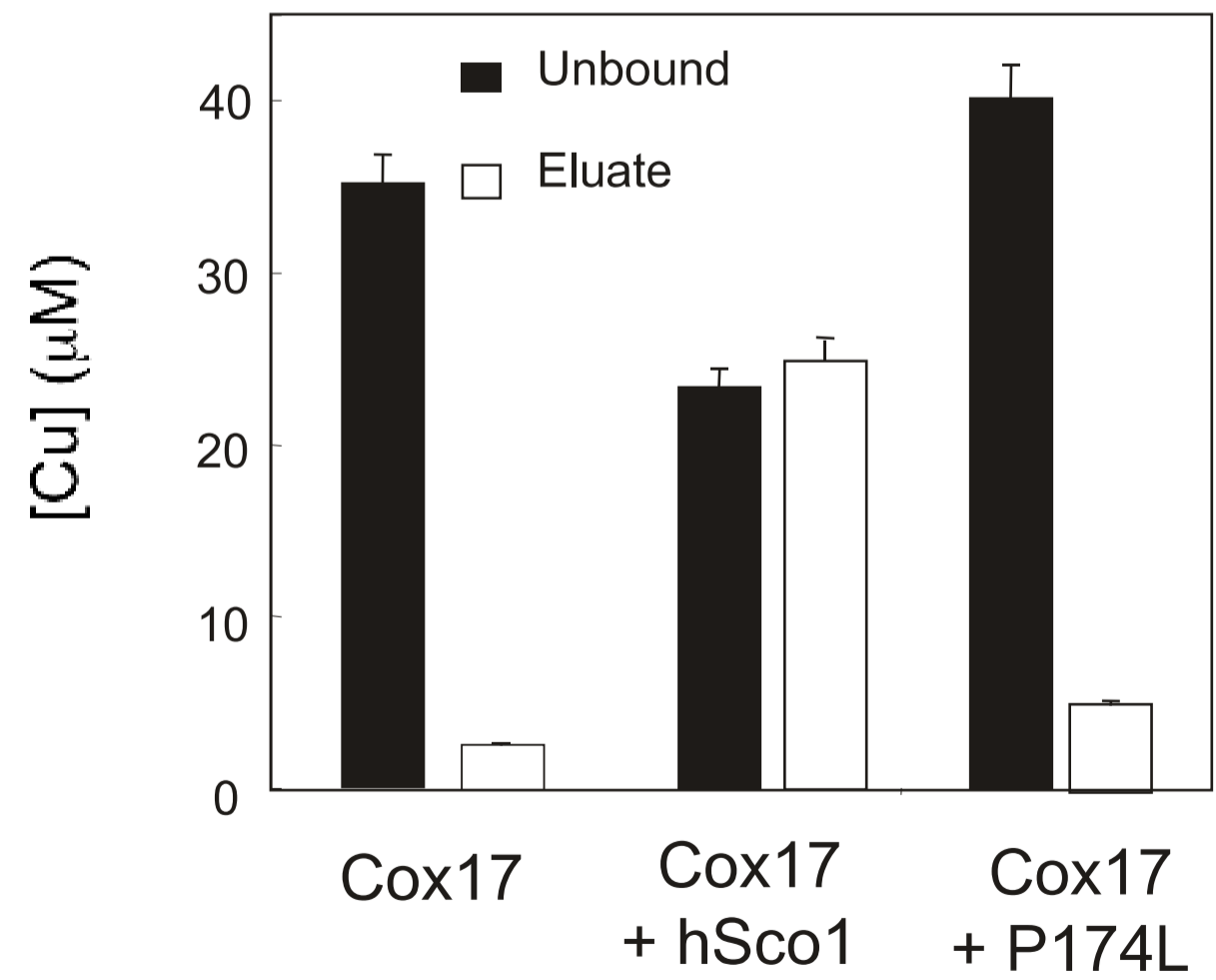


Fig.5C

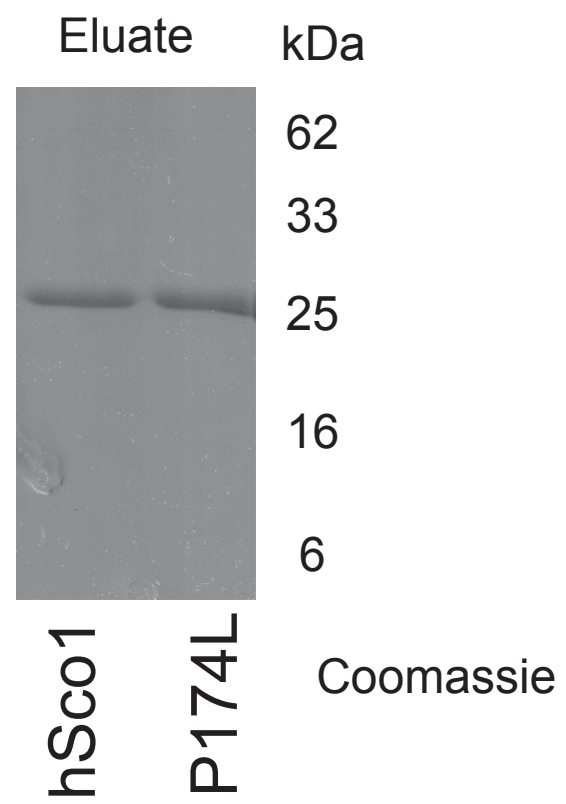


Fig. 5D

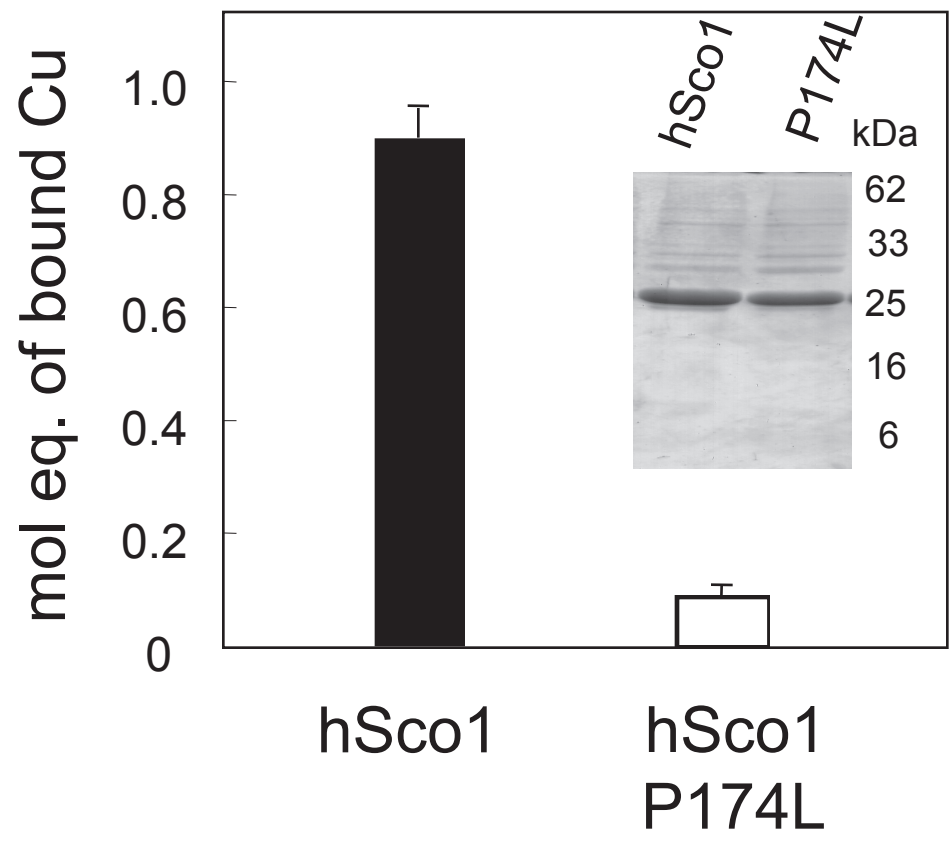


Fig.6

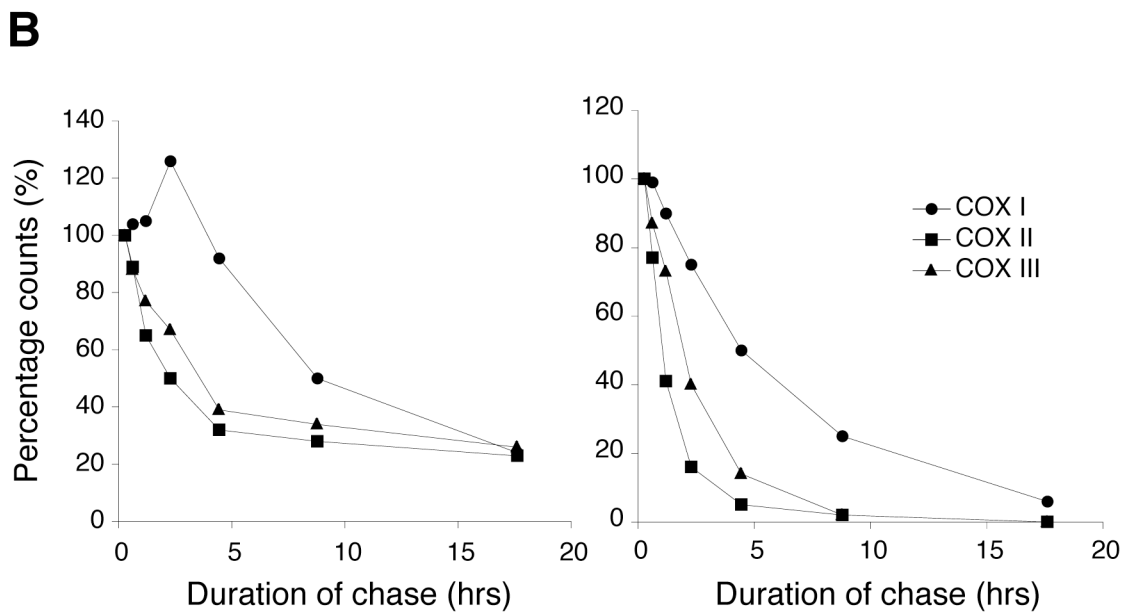
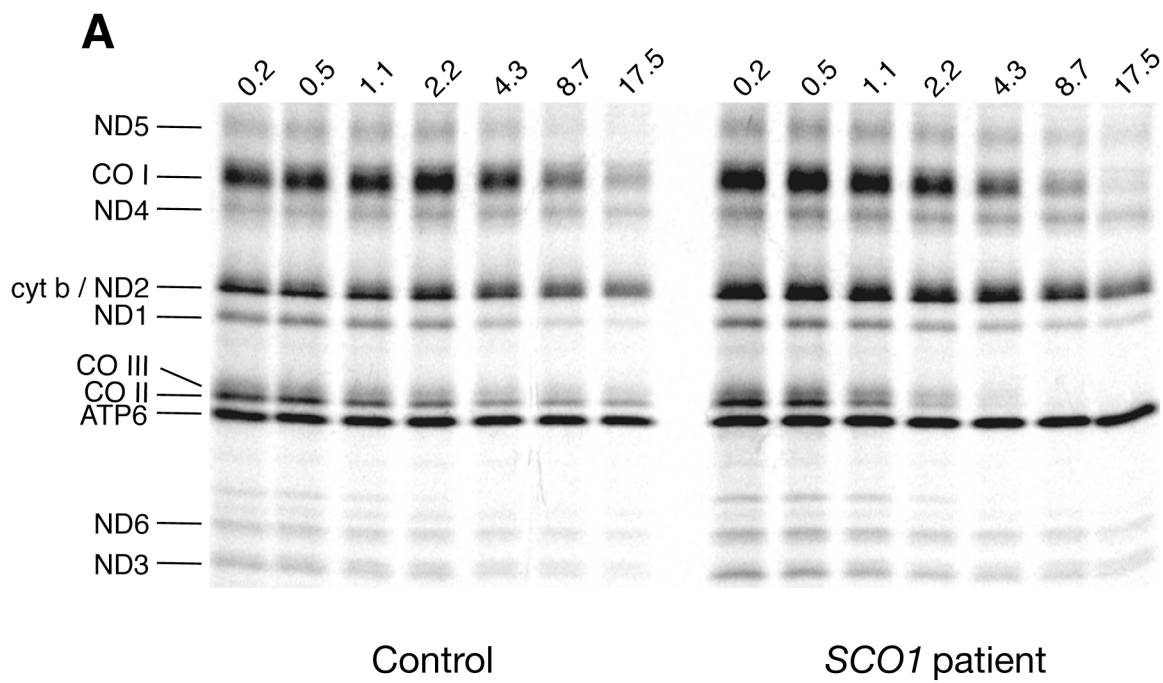
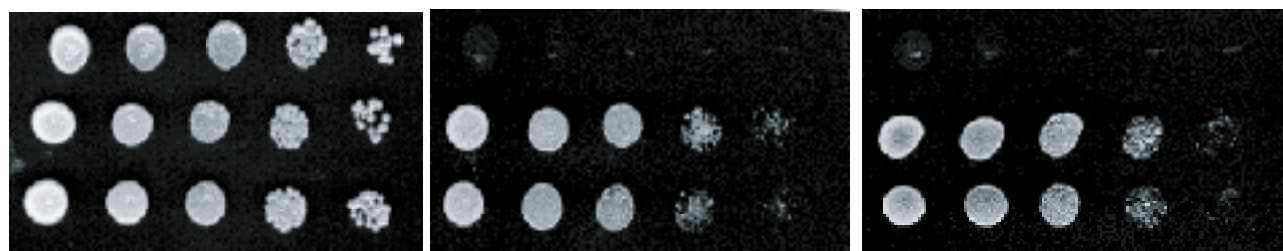


Figure 7

*sco1*Δ

+VEC
+YCp *scoSCO1*
+YCp *scoP153L*



-His
Glucose

-His
Lac-Gly

-His
Lac-Gly
1mM Cu

Fig.8

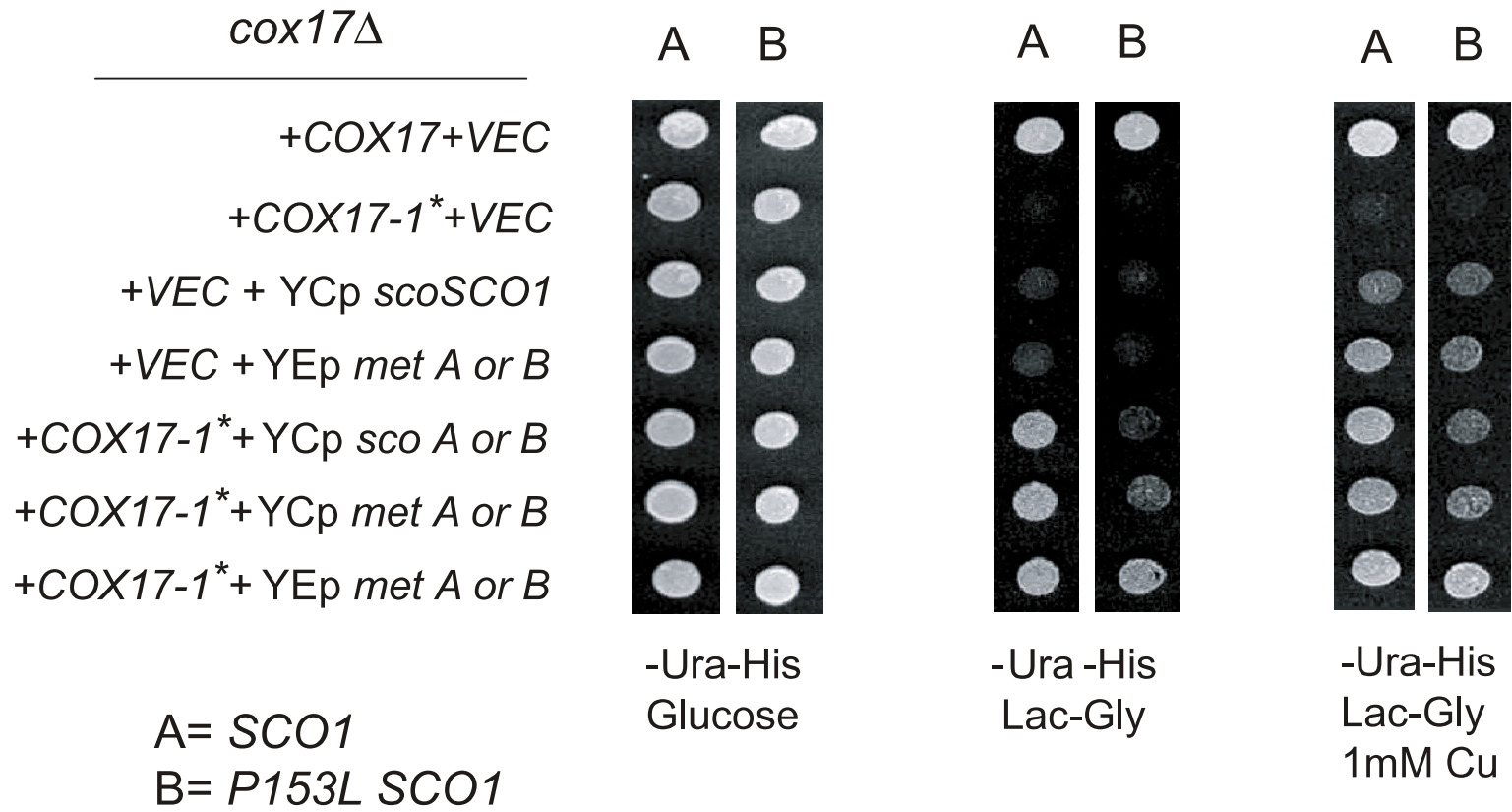


Fig.9A

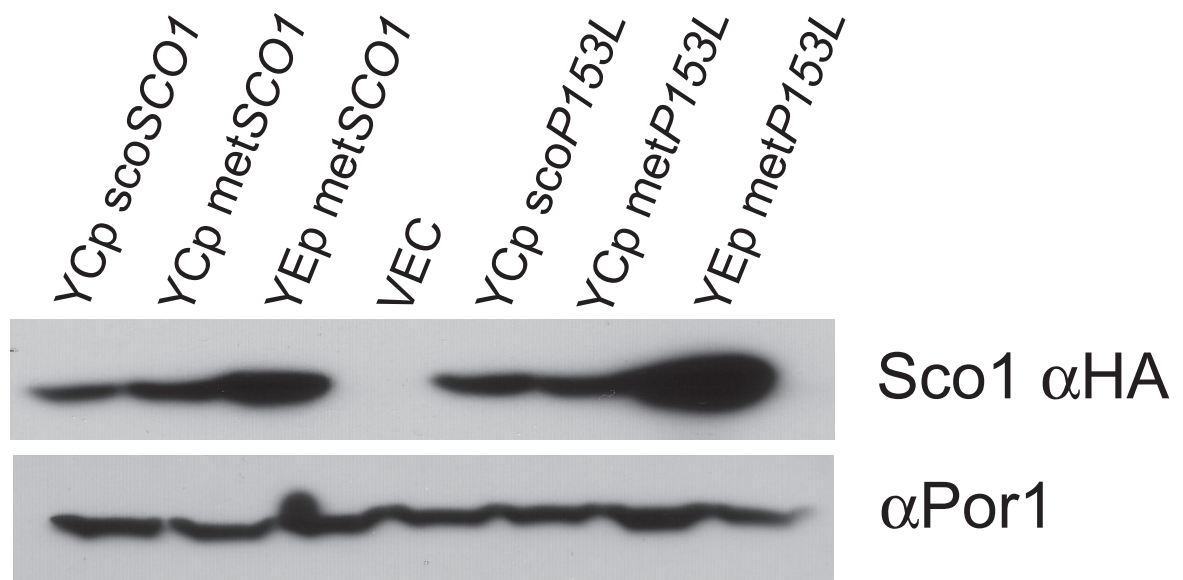


Fig. 9B